Formation of Semi-Covalent Bond in $[(N_2O)_nH_2O]^+$ (n = 2–7) Cluster Ions Studied by IR Spectroscopy

Ryoko Matsushima, Takayuki Ebata, and Yoshiya Inokuchi[a)]

Department of Chemistry, Graduate School of Science, Hiroshima University

Higashi-Hiroshima, Hiroshima 739-8526, Japan

ABSTRACT

IR photodissociation (IRPD) spectra of $[(N_2O)_nH_2O]^+$ with n = 2–7 are measured in the 1100–3800 cm^{-1} region. In parallel, the geometry optimization and the vibrational analysis are carried out at the B3LYP/6-311++G(d,p) level of theory. In the OH stretching (2400–3800 cm^{-1}) region, the IRPD spectrum of the $[(N_2O)_2H_2O]^+$ ion shows a sharp band at 3452 cm^{-1} and a broad one at around 2700 cm^{-1}, which are assignable to the stretching vibrations of the free and hydrogen-bonded OH groups, respectively. The IRPD spectra of the $[(N_2O)_nH_2O]^+$ (n = 3–7) ions show no band of the free OH stretching vibration, indicating that both of the OH groups are hydrogen-bonded to solvent N_2O molecules. The IRPD spectra of the n = 2–7 ions also show the ν_1 and ν_3 vibrations of the N_2O components at around 1250 and 2200 cm^{-1}, respectively. Comparison of the IRPD spectra with the calculated IR spectra suggests that the $[(N_2O)_nH_2O]^+$ cluster ions have an $(N_2O \cdot H_2O)^+$ ion core, in which the positive charge is delocalized over the H_2O and N_2O components, and that an intermolecular semi-covalent bond is formed between the oxygen atoms of H_2O and N_2O through the charge resonance interaction.

[a)]Author to whom correspondence should be addressed (y-inokuchi@hiroshima-u.ac.jp).

1. INTRODUCTION

In molecular clusters consisting of a radical ion and closed-shell molecules, the charge resonance (CR) interaction frequently controls the charge distribution and the cluster structure. The CR interaction occurs by the interference between the singly-occupied molecular orbital (SOMO) of a radical ion and the highest-occupied MO (HOMO) of a molecule. As a result, a semi-covalent bond is formed between the radical ion and the molecule, and the charge is delocalized over the components. One of the straightforward investigations for the CR interaction in molecular cluster ions is the observation of the CR transition in the visible region. Actually, a number of cluster systems have been studied by absorption spectroscopy both in condensed phase and in the gas phase.[1–12] However, the CR transition does not provide so much information on the cluster structure, because the CR band has intrinsically a broad nature, showing no vibronic transition. In the last decade, we have applied IR photodissociation (IRPD) spectroscopy to the cluster systems in which the CR interaction may occur. Recently our attention lies on the cluster ions of triatomic molecules such as CO_2, CS_2, OCS, and N_2O.[13–15] These molecules have very strong transitions in the 1000–2500 cm^{-1} region that are due to the stretching vibrations, and IR spectra in this region show useful information on the structure.

The target systems in this study are the $[(N_2O)_nH_2O]^+$ ions. Bowers and co-workers studied the photodissociation dynamics of the $(N_2O \cdot H_2O)^+$ ion in the visible region.[16] They concluded that two stable isomers involve in the photodissociation. One is a structure with an N_2O^+ ion core, $N_2O^+ \bullet\bullet\bullet H_2O$; the H_2O molecule is bound through its oxygen atom, midway between the central nitrogen atom and the terminal oxygen atom of the N_2O^+ ion core. The other one has a proton transferred form, $N_2OH^+ \bullet\bullet\bullet OH$, in which the positive charge is localized in the N_2OH part. In their quantum chemical calculations at the HF and the MP2 levels, the $N_2OH^+ \bullet\bullet\bullet OH$ structure is more stable than the $N_2O^+ \bullet\bullet\bullet H_2O$ one by more than 10

kcal/mol. Dressler and co-workers reported collision-induced dissociation (CID) and photodissociation (PD) measurements of the $(N_2O\cdot H_2O)^+$ ion.[17–19] They suggested that all the fragment ions due to CID and PD originate from the same $(N_2O\cdot H_2O)^+$ structure, although they did not determine definitely the structure or the charge distribution of the $(N_2O\cdot H_2O)^+$ ion. Theoretically, Morokuma and co-workers reported the potential energy surface of the $(N_2O\cdot H_2O)^+$ ion.[20] They optimized the geometry of the $(N_2O\cdot H_2O)^+$ ion with the B3LYP functional and found two isomers that are stabilized by a donative interaction of a lone pair on the water oxygen atom with a SOMO of the N_2O component. From the comparison of the calculation results with the experimental ones, they suggested that only one of the two isomers, which has an intermolecular bond between the oxygen atoms of H_2O and N_2O, might exist in the previous CID and PD experiments. Meanwhile, there has been no report for the $[(N_2O)_nH_2O]^+$ cluster ions. These cluster ions are isoelectric with the $[(CO_2)_nH_2O]^+$ ions, which we have studied by IRPD spectroscopy.[21] In the $[(CO_2)_nH_2O]^+$ ions, the positive charge is localized on the H_2O moiety, because the ionization potential (IP) of H_2O (12.62 eV) is much lower than that of CO_2 (13.78 eV).[22] In the case of the $[(N_2O)_nH_2O]^+$ ions, the IP of N_2O is 12.89 eV, which is higher than that of H_2O only by 0.27 eV.[22] Therefore, the charge distribution in the $[(N_2O)_nH_2O]^+$ ions will be quite different from that in the $[(CO_2)_nH_2O]^+$ ions.

In the present study, we investigate the charge distribution and the solvation structure for the $[(N_2O)_nH_2O]^+$ cluster ions with n = 2–7 by IRPD spectroscopy. The IRPD spectra are measured in the 1100-3800 cm^{-1} region. These clusters will exhibit IR bands assignable to the symmetric and anti-symmetric stretching vibrations (ν_1 and ν_3) of N_2O in the 1100–2400 cm^{-1} region and the OH stretching vibration of H_2O in the 2400–3800 cm^{-1} region. In order to assign the IRPD spectra, we carry out the geometry optimization and the vibrational analysis of several species at the B3LYP/6-311++G(d,p) level of theory.

Comparing the IRPD spectra with the IR spectra predicted by quantum chemical calculations, we provide definite structures for these cluster ions.

2. EXPERIMENTAL AND COMPUTATIONAL

The details of our experiment have been given elsewhere.[13, 14] A mixture of pure N_2O gas and water vapor is injected into a source chamber through a pulsed nozzle with a stagnation pressure of 0.3 MPa. The pulsed free jet crosses an electron beam at the exit of the nozzle with an electron kinetic energy of 350 eV, producing $[(N_2O)_nH_2O]^+$. Cluster ions produced are accelerated into a flight tube by applying pulsed electric potential (~1.3 kV) to Wiley-McLaren type acceleration grids. In the flight tube, only target parent ions can go through a mass gate. After passing through the gate, the mass-selected parent ions are irradiated by an output of a pulsed IR laser. Resultant fragment ions are mass analyzed by a reflectron mass spectrometer and detected by a multichannel plate (MCP). An output from the MCP is amplified by a commercial amplifier and fed into a digital storage oscilloscope. Yields of fragment ions are normalized by the intensity of parent ions and the photodissociation laser. IRPD spectra of parent ions are obtained by plotting normalized yields of fragment ions against wavenumber of the IR laser. The fragmentation channel detected for the IRPD spectra of the $[(N_2O)_nH_2O]^+$ ions is the loss of one N_2O molecule. The tunable IR light in the 2000–3800 cm^{-1} region is an idler output of an optical parametric oscillator (OPO) (LaserVision) pumped by a fundamental output of a Nd:YAG (neodymium-doped yttrium aluminum garnet) laser (Spectra Physics GCR250). We obtain the IR laser in the 1100–2300 cm^{-1} region by using different frequency generations between the idler and the signal outputs of the OPO laser with a $AgGaSe_2$ crystal.

In order to analyze the IRPD spectra, we carry out density functional theory (DFT)

calculations with the GAUSSIAN03 program package.[23] The geometry optimization and the vibrational analysis are done at the B3LYP/6-311++G(d,p) level of theory. For comparison of the IRPD spectra with calculated IR spectra, a scaling factor of 0.9464 is employed to vibrational frequencies calculated. This factor is determined so as to reproduce the frequency of the ν_1 (1285.0 cm^{-1}) and ν_3 (2223.5 cm^{-1}) vibrations of neutral N_2O monomer.[24]

3. RESULTS AND DISCUSSION

A. IRPD spectra of $[(N_2O)_nH_2O]^+$ (n = 2–7)

Figure 1 shows the IRPD spectra of the $[(N_2O)_nH_2O]^+$ (n = 2–7) ions in the 1100–3800 cm^{-1} region. The $(N_2O \cdot H_2O)^+$ ion is not photodissociated in this frequency region, indicating that the n = 1 ion has a binding energy larger than that of the n = 2–7 ions. Band positions of the IRPD spectra are collected in Table 1. The IR absorption in the 2400–3800 cm^{-1} region can be assigned to the OH stretching vibration of the H_2O component. For all the clusters of n = 2–7, there is a quite broad band at around 2700 cm^{-1}, which is attributed to the stretching vibration of the hydrogen-bonded OH group. In the n = 2 spectrum, a sharp band is observed at 3452 cm^{-1}, which is ascribed to the free OH stretching vibration. Thus, for the n = 2 ion, one of the two OH groups is hydrogen-bonded to the N_2O molecule(s), and the other one is free from the intermolecular bond. The result of the $[(N_2O)_2H_2O]^+$ ion is contrastive to that of the $[(CO_2)_2H_2O]^+$ ion; the positive charge is localized in the H_2O component, and both of the OH groups of the H_2O^+ ion core are hydrogen-bonded to one CO_2 molecule each.[21] Moreover, the stretching vibration of the free OH group in the $[(N_2O)_2H_2O]^+$ ion has an intermediate frequency (3452 cm^{-1}) between the OH stretching frequencies of H_2O and H_2O^+; the frequencies of the symmetric and anti-symmetric OH stretching vibrations are 3657.1 and 3755.8 cm^{-1} for H_2O monomer[24] and

3182.7 and 3219.5 cm^{-1} for H_2O^+ monomer ion.[25] This result indicates that a part of the positive charge is distributed on the H_2O component in the $[(N_2O)_2H_2O]^+$ ion, but an H_2O^+ ion core is not completely formed different from the $[(CO_2)_2H_2O]^+$ ion. For the n = 3–7 ions, both of the OH groups are hydrogen-bonded to the N_2O molecules.

In addition to the OH bands, all the IRPD spectra in Fig. 1 display bands at around 1250 and 2230 cm^{-1}, which can be assigned to the ν_1 and ν_3 vibrations of N_2O components in the $[(N_2O)_nH_2O]^+$ clusters. Figure 2a shows expanded views of the IRPD spectra around the ν_1 vibration of N_2O. The n = 2 ion shows a very broad feature; probably only a very hot part of the n = 2 ions can contribute to the photodissociation in the 1100–1300 cm^{-1} region. For the n = 3 ion, two bands are clearly observed at 1193 and 1246 cm^{-1}. In the case of the n = 4 ion, another component appears as a shoulder around 1266 cm^{-1} (highlighted with an arrow in Fig. 2a) in addition to the two bands at 1208 and 1245 cm^{-1}. For the n = 5–7 clusters, the intensity of the band at ~1275 cm^{-1} increases relative to that of the bands at ~1220 and ~1250 cm^{-1} with increasing the cluster size. The band position of the higher-frequency component (~1275 cm^{-1}) is more close to that of the ν_1 vibration of N_2O (1285.0 cm^{-1}). Therefore, the higher-frequency band around 1275 cm^{-1} can be ascribed to solvent N_2O molecules that have weaker interaction with the ion core. In the 2000–2300 cm^{-1} region (Fig. 2b), there are two bands at around 2180 and 2230 cm^{-1}. The lower-frequency band shifts to higher frequency from 2147 cm^{-1} (n = 2) to 2195 cm^{-1} (n = 7), whereas the higher-frequency band is located at almost the same position around 2230 cm^{-1}. For the n = 3–7 ions, the integrated intensity of the higher-frequency band relative to the lower-frequency one seems to increase with increasing the cluster size. Therefore, the ~2230 cm^{-1} band can be ascribed to the ν_3 vibration of solvent N_2O molecules. For the definitive assignment of the IRPD bands in the 1100–2300 cm^{-1} region, however, the result of the quantum chemical calculation seems to be indispensable.

B. Structure of $[(N_2O)_nH_2O]^+$ clusters

The IRPD result of the $[(N_2O)_2H_2O]^+$ ion suggests that one of the OH groups is free from the intermolecular bond, and the positive charge is partly occupied by the H_2O component. In order to determine the ion core in the $[(N_2O)_nH_2O]^+$ ions, we first carry out the geometry optimization of the $(N_2O \cdot H_2O)^+$ ion at the B3LYP/6-311++G(d,p) level of theory. We obtain two stable isomers, 1A and 1B (Fig. 3). In both structures, the positive charge is delocalized over the two molecules; no isomer with the H_2O^+ or N_2O^+ ion core is found in our calculations. The most stable structure is isomer 1A; the oxygen atom of the H_2O part is bound to the oxygen end of the N_2O component. In isomer 1B, the oxygen atom of H_2O is bonded to the terminal nitrogen of N_2O. Isomer 1A is more stable than isomer 1B by 760 cm^{-1}; this stability order agrees with the previous theoretical results.[20] In addition, the structure of isomer 1A is essentially the same as that of the form which was predicted to exist in the previous CID and PD experiments of the $(N_2O \cdot H_2O)^+$ ion.[20] Therefore, it is quite probable that isomer 1A is the ion core in the $[(N_2O)_nH_2O]^+$ cluster ions. Figure 3c displays a representative of intermolecular bonding MOs between the H_2O and N_2O components in isomer 1A. This MO is formed by the constructive interference between the HOMOs of H_2O and N_2O. As a result of the CR interaction between the H_2O and N_2O components, a covalent bond with a bond order of 0.5, called a "semi-covalent" bond, is formed between them. The binding energies of isomers 1A and 1B to H_2O^+ and neutral N_2O are calculated to be 12021 and 11261 cm^{-1}, respectively. These values are lower than the binding energy of a single covalent bond formed between oxygen atoms (for instance, the binding energy of HO–OH of H_2O_2 is ~17800 cm^{-1}), but much higher than that of the intermolecular bond with the electrostatic interaction (a few thousands of cm^{-1}).

The predominance of isomer 1A over 1B as the ion core emerges also in the

geometry optimization of the $[(N_2O)_2H_2O]^+$ ion. Figure 4 shows the IRPD spectrum, the structure of four most stable isomers, and their IR spectra of the $[(N_2O)_2H_2O]^+$ ion. The relative energy, binding energy, vibrational frequency, and IR intensity are collected in Table 2. The most stable isomer (2A) has an $(N_2O\cdot H_2O)^+$ ion core similar to isomer 1A. Isomer 2C also has a 1A-like ion core. Both of isomers 2A and 2C have an O–H···N_2O hydrogen bond. The difference in the structure between 2A and 2C is the orientation of the solvent N_2O molecule to the ion core; in isomer 2A the solvent N_2O molecule is bonded to the $(N_2O\cdot H_2O)^+$ ion core at the oxygen end, whereas at the nitrogen end in 2C. In isomer 2D, the ion core is also an $(N_2O\cdot H_2O)^+$ ion, but it is similar to isomer 1B. Isomer 2D is less stable than 2A and 2C by ~700 cm^{-1}; this value is almost the same as the difference in the total energy between 1A and 1B. Therefore, the 1A-like ion core is more likely to exist in the $[(N_2O)_nH_2O]^+$ cluster ions. Isomer 2B shows a similar stability to 2A and 2C. Both of the N_2O components are bound to the oxygen atom of the H_2O part, and the positive charge is delocalized over the three molecules. In our calculations, no isomer is found having an $(N_2O)_2^+$ ion core, which is the ion core in the $(N_2O)_n^+$ homocluster ions.[15] Comparison of the IRPD spectrum with the IR spectra of 2A–2D provides the structural assignment of the $[(N_2O)_2H_2O]^+$ ion. First, we can exclude isomer 2B for the structure of $[(N_2O)_2H_2O]^+$, because 2B does not reproduce the hydrogen-bonded OH band. Isomers 2A, 2C, and 2D show similar IR spectra in the OH stretching region. The difference in the spectral feature for 2A, 2C, and 2D emerges in the 1100–2400 cm^{-1} region. Isomers 2A, 2C, and 2D have two ν_3 vibrations of the N_2O component in the 2000–2300 cm^{-1} region. The low- and high-frequency bands are due to the N_2O component in the $(N_2O\cdot H_2O)^+$ ion core and the solvent N_2O molecule, respectively. For 2A and 2C, the low-frequency band is weaker than the high-frequency one, whereas the former band is stronger than the latter for 2D. As seen in Fig. 4a, the relative intensity of the two IRPD bands of $[(N_2O)_2H_2O]^+$ at 2147 and 2232

cm^{-1} shows a very good agreement with that of isomers 2A and 2C. Therefore, the structure of the $[(N_2O)_2H_2O]^+$ ion can be assigned to 2A and/or 2C. For the ν_1 vibration of the N_2O component, isomer 2A has two bands with similar intensity (Fig. 4b), while one of the two ν_1 bands is much weaker than the other for 2C (Fig. 4d). However, the observed IRPD spectrum of the $[(N_2O)_2H_2O]^+$ in the 1100–1500 cm^{-1} region does not clearly agree either with 2A or 2C due to the broad spectral feature. Further assignment for the $[(N_2O)_2H_2O]^+$ ion is not possible by the comparison of the IR spectra.

A similar relationship between the stability and the cluster structure is seen for the $[(N_2O)_3H_2O]^+$ ion. In the geometry optimization of the $[(N_2O)_3H_2O]^+$ ion, six stable isomers are obtained; no isomer with an $(N_2O)_2^+$ ion core is found also for the $[(N_2O)_3H_2O]^+$ ion. Figure 5 shows the IRPD spectrum, the optimized structure and the IR spectra of the four most stable isomers of the $[(N_2O)_3H_2O]^+$ ion. The relative energy, binding energy, vibrational frequency, and IR intensity are displayed in Table 3. The three most stable structures (3A–3C) have an $(N_2O\cdot H_2O)^+$ ion core similar to isomer 1A. The fourth to sixth stable isomers have a 1B-type ion core. These isomers are less stable than the first to third stable isomers by ~700 cm^{-1}. Therefore, it is quite probable that the $[(N_2O)_3H_2O]^+$ ion also has a 1A-type $(N_2O\cdot H_2O)^+$ ion core, similar to the case of the $[(N_2O)_2H_2O]^+$ ion. As seen in Fig. 5, the IR spectra of 3A–3C agree with the IRPD spectrum of the $[(N_2O)_3H_2O]^+$ ion in the region of 2300–3800 cm^{-1}; the symmetric and anti-symmetric stretching vibrations of the hydrogen-bonded OH groups strongly appear around 3000 cm^{-1}. In the region of the ν_3 vibration of N_2O (2000–2300 cm^{-1}), there are three bands; the lowest-frequency band is due to the N_2O component in the $(N_2O\cdot H_2O)^+$ ion core. The two bands assignable to the solvent N_2O molecules are close to each other, providing only one band maximum. As a result, isomers 3A–3C show two band maxima in the 2000–2300 cm^{-1}. This spectral feature of 3A–3C is similar to the IRPD spectrum in the 2000–2300 cm^{-1} region that two bands are

observed at 2173 and 2235 cm^{-1}. It is difficult to assign the structure of the $[(N_2O)_3H_2O]^+$ ion to either of isomers 3A–3C by the IR spectra in the 2000–3800 cm^{-1} region. In the 1100–1300 cm^{-1} region, isomers 3A–3C show different spectral feature from each other. The N_2O component of the $(N_2O\cdot H_2O)^+$ ion core provides the ν_1 vibration at almost the same (~1157 cm^{-1}) position for 3A–3C. However, the band position and the intensity for the solvent N_2O molecules are strongly dependent on the solvation manner to the $(N_2O\cdot H_2O)^+$ ion core. In isomer 3A, both of the solvent N_2O molecules are bonded to the H_2O component at the oxygen end, and show the ν_1 vibrations at 1219 and 1221 cm^{-1}. In the case of isomer 3B, the solvent N_2O molecule bound to the ion core at the oxygen end has the ν_1 band at 1219 cm^{-1}, whereas the N_2O component bonded at the terminal nitrogen shows a weak ν_1 band at 1323 cm^{-1}. For isomer 3C, in which both of the solvent N_2O molecules form intermolecular bonds at the nitrogen end, there are two weak ν_1 bands at 1323 cm^{-1}. The IRPD spectrum of the $[(N_2O)_3H_2O]^+$ ion shows two comparable bands at 1193 and 1246 cm^{-1}, but no band is observed at around 1320 cm^{-1}. As a result, we can assign the structure of the $[(N_2O)_3H_2O]^+$ ion to isomer 3A. In conclusion, the $[(N_2O)_3H_2O]^+$ ion has an $(N_2O\cdot H_2O)^+$ ion core like isomer 1A, and both of the OH groups are hydrogen-bonded to one N_2O molecule each; the solvent N_2O molecules are bonded to the ion core at the oxygen end.

Since isomer 3A is the structure for the $[(N_2O)_3H_2O]^+$ ion, it seems reasonable that the $[(N_2O)_4H_2O]^+$ ion is formed on this isomer. Figure 6 shows a representative of the $n = 4$ isomers with a 3A-like structure. In this structure, the fourth N_2O molecule is bonded to the $(N_2O\cdot H_2O)^+$ ion core of the 3A part. The intermolecular interaction between the fourth N_2O molecule and the 3A part is smaller than that in the $[(N_2O)_3H_2O]^+$ ion; the binding energy of 4A to 3A and N_2O is 1775 cm^{-1}, whereas that of 3A to 2A and N_2O is 2725 cm^{-1} (see Table 4). The vibrational analysis of 4A shows that the ν_1 vibration of the fourth N_2O molecule has a frequency (1238 cm^{-1}) higher than that of the other solvent N_2O molecules at the OH

groups (1222 and 1224 cm^{-1}). This result agrees well with the IRPD result of the $[(N_2O)_4H_2O]^+$ ion that the third band appears at 1266 cm^{-1} in the N_2O ν_1 region. As seen in Fig. 2a, the spectral feature that there are three bands in the ν_1 vibrational region is almost the same for the n = 4–7 ions, although the relative intensity and the position of the three bands change with the cluster size. Therefore, it is probable that there is a component similar to 3A and the fourth to seventh N_2O molecules are weakly bonded to the component in the $[(N_2O)_nH_2O]^+$ (n = 4–7) ions.

4. SUMMARY

The IR photodissociation spectra (IRPD) of $[(N_2O)_nH_2O]^+$ with n = 2–7 were measured in the 1100–3800 cm^{-1} region. The geometry optimization and the vibrational analysis were also carried out for the $[(N_2O)_nH_2O]^+$ (n = 1–4) ions at the B3LYP/6-311++G(d,p) level of theory. All the IRPD bands can be attributed to the $(N_2O\cdot H_2O)^+$ ion core and the solvent N_2O molecules. The $(N_2O\cdot H_2O)^+$ ion core has a semi-covalent bond between the oxygen atoms of the N_2O and H_2O components through the charge resonance (CR) interaction. As a result, the positive charge is delocalized over the N_2O and H_2O molecules. The IRPD spectra of the $[(N_2O)_2H_2O]^+$ ion shows the free and hydrogen-bonded OH stretching bands of the $(N_2O\cdot H_2O)^+$ ion core. No free OH stretching band is found for the $[(N_2O)_3H_2O]^+$ ion, indicating that both of the OH groups are hydrogen-bonded to one N_2O molecule each. In addition to the OH stretching bands, the IRPD spectra show the ν_1 and ν_3 vibrations of the N_2O components at ~1250 and ~2230 cm^{-1}. The N_2O component in the $(N_2O\cdot H_2O)^+$ ion shows the ν_1 and ν_3 bands at frequencies lower than those of the solvent N_2O molecules. From the spectral features in the ν_1 and ν_3 vibrational regions, we conclude that two solvent N_2O molecules are strongly bonded to the

OH groups of the $(N_2O \cdot H_2O)^+$ ion core, and that further N_2O molecules are more weakly attached to the $(N_2O \cdot H_2O)^+$ ion.

ACKNOWLEDGMENT

This work is supported by Grant-in-Aids (Grant Nos. 18205003 and 21350016) for Scientific Research from the Ministry of Education, Culture, Sports, Science, and Technology (MEXT).

REFERENCES

[1] Badger, B.; Broklehurst, B. *Nature* **1968**, *219*, 263.

[2] Shida, T.; Hamill, W. H. *J. Chem. Phys.* **1966**, *44*, 4372.

[3] Shkrob, I. A.; Sauer, Jr., M. C.; Jonah, C. D.; Takahashi, K. *J. Phys. Chem. A* **2002**, *106*, 11855.

[4] Jarrold, M. F.; Illies, A. J.; Bowers, M. T. *J. Chem. Phys.* **1983**, *79*, 6086.

[5] Jarrold, M. F.; Illies, A. J.; Bowers, M. T. *J. Chem. Phys.* **1984**, *81*, 214.

[6] Illies, A. J.; Jarrold, M. F.; Wagner-Redeker, W.; Bowers, M. T. *J. Phys. Chem.* **1984**, *88*, 5204.

[7] Jarrold, M. F.; Illies, A. J.; Bowers, M. T. *J. Chem. Phys.* **1985**, *82*, 1832.

[8] Snodgrass, J. T.; Dunbar, R. C.; Bowers, M. T. *J. Phys. Chem.* **1990**, *94*, 3648.

[9] Jarrold, M. F.; Illies, A. J.; Bowers, M. T. *J. Chem. Phys.* **1985**, *81*, 4882.

[10] Ohashi, K.; Nishi, N. *J. Chem. Phys.* **1991**, *95*, 4002.

[11] Ohashi, K.; Nishi, N. *J. Phys. Chem.* **1992**, *96*, 2931.

[12] Ohashi, K.; Nakai, Y.; Shibata, T.; Nishi, N. *Laser Chem.* **1994**, *14*, 3.

[13] Kobayashi, Y.; Inokuchi, Y.; Ebata, T. *J. Chem. Phys.* **2008**, *128*, 164319.

[14] Inokuchi, Y.; Muraoka, A.; Nagata, T.; Ebata, T. *J. Chem. Phys.* **2008**, *129*, 044308.

[15] Inokuchi, Y.; Matsushima, R.; Kobayashi, Y.; Ebata, T. *J. Chem. Phys.* **2009**, *131*, 044325.

[16] Graul, S. T.; Kim, H.-S.; Bowers, M. T. *Int. J. Mass Spectrom. Ion Proc.* **1992**, *117*, 507.

[17] Bastian, M. J.; Dressler, R. A.; Levandier, D. J.; Murad, E.; Muntean, F.; Armentrout, P. B. *J. Chem. Phys.* **1997**, *106*, 9570.

[18] Williams, S.; Chiu, Y.-H.; Levandier, D. J.; Dressler, R. A. *J. Chem. Phys.* **1998**, *108*, 9383.

[19] Williams, S.; Chiu, Y.-H.; Levandier, D. J.; Dressler, R. A. *J. Chem. Phys.* **1998**, *109*, 7450.

[20] Stevens, J. E.; Holthausen, M. C.; Morokuma, K. *J. Chem. Phys.* **1999**, *111*, 7766.

[21] Inokuchi, Y.; Kobayashi, Y.; Muraoka, A.; Nagata, T.; Ebata, T. *J. Chem. Phys.* **2009**, *130*, 154304.

[22] Kimura, K.; Katsumata, S.; Achiba, Y.; Yamazaki, T.; Iwata, S. *Handbook of HeI Photoelectron Spectra of Fundamental Organic Molecules* (Japan Scientific Societies, Tokyo, 1981).

[23] Frisch, M. J.; Trucks, G. W.; Schlegel, H. B.; Scuseria, G. E.; Robb, M. A.; Cheeseman, J. R.; Montgomery, Jr., J. A.; Vreven, T.; Kudin, K. N.; Burant, J. C.; Millam, J. M.; Iyengar, S. S.; Tomasi, J.; Barone, V.; Mennucci, B.; Cossi, M.; Scalmani, G.; Rega, N.; Petersson, G. A.; Nakatsuji, H.; Hada, M.; Ehara, M.; Toyota, K.; Fukuda, R.; Hasegawa, J.; Ishida, M.; Nakajima, T.; Honda, Y.; Kitao, O.; Nakai, H.; Klene, M.; Li, X.; Knox, J. E.; Hratchian, H. P.; Cross, J. B.; Adamo, C.; Jaramillo, J.; Gomperts, R.; Stratmann, R. E.; Yazyev, O.; Austin, A. J.; Cammi, R.; Pomelli, C.; Ochterski, J. W.; Ayala, P. Y.; Morokuma, K.; Voth, G. A.; Salvador, P.; Dannenberg, J. J.; Zakrzewski, V. G.; Dapprich, S.; Daniels, A. D.; Strain, M. C.; Farkas, O.; Malick, D. K.; Rabuck, A. D.; Raghavachari, K.; Foresman, J. B.; Ortiz, J. V.; Cui, Q.; Baboul, A. G.; Clifford, S.; Cioslowski, J.; Stefanov, B. B.; Liu, G.; Liashenko, A.; Piskorz, P.; Komaromi, I.; Martin, R. L.; Fox, D. J.; Keith, T.; Al-Laham, M. A.; Peng, C. Y.; Nanayakkara, A.; Challacombe, M.; Gill, P. M. W.; Johnson, B.; Chen, W.; Wong, M. W.; Gonzalez, C.; Pople, J. A. Gaussian 03, Rev. C.02, Gaussian, Inc., Wallingford CT, 2004.

[24] Herzberg, G. *Molecular Spectra and Molecular Structure: Infrared and Raman Spectra of Polyatomic Molecules* (Krieger, Malabar, 1991), Vol.2.

[25] Forney, D.; Jacox, M. E.; Thompson, W. E. *J. Chem. Phys.* **1993**, *98*, 841.

Table 1. Band positions (cm^{-1}) and assignment of the IRPD spectra of $[(N_2O)_nH_2O]^+$.

$n = 2$	$n = 3$	$n = 4$	$n = 5$	$n = 6$	$n = 7$	Assignment
–	1193	1208	1216	1221	1224	ν_1 [N_2O in $(N_2O{\bullet}H_2O)^+$]
–	1246	1245	1249	1251	1253	ν_1 (solvent N_2O)
–	–	1266	1272	1275	1278	ν_1 (solvent N_2O)
2147	2173	2188	2190	2192	2195	ν_3 [N_2O in $(N_2O{\bullet}H_2O)^+$]
2232	2235	2232	2232	2232	2232	ν_3 (solvent N_2O)
~2700	~2700	~2700	~2700	~2700	~2700	H-bonded OH
3452	–	–	–	–	–	free OH

Table 2. Relative energies, binding energies, vibrational frequencies, IR intensities, and assignment for optimized isomers of $[(N_2O)_2H_2O]^+$.

Isomer	Relative Energy[a] (cm^{-1})	Binding Energy[a] (cm^{-1})	Frequency[b] (cm^{-1})	IR intensity (km/mol)	Assignment
2A	(0)	3226	1144	108	ν_1 [N_2O in $(N_2O{\bullet}H_2O)^+$]
			1214	200	ν_1 (solvent N_2O)
			1482	71	H_2O bending
			2121	74	ν_3 [N_2O in $(N_2O{\bullet}H_2O)^+$]
			2247	406	ν_3 (solvent N_2O)
			2990	1983	H-bonded OH
			3473	363	free OH
2B	28	3198	1189	242	ν_1 (N_2O)
			1192	100	
			1495	76	H_2O bending
			2144	170	ν_3 (N_2O)
			2150	138	
			3442	201	free OH
			3547	206	
2C	83	3144	1144	110	ν_1 [N_2O in $(N_2O{\bullet}H_2O)^+$]
			1329	18	ν_1 (solvent N_2O)
			1484	68	H_2O bending
			2124	86	ν_3 [N_2O in $(N_2O{\bullet}H_2O)^+$]
			2265	861	ν_3 (solvent N_2O)
			2949	2103	H-bonded OH
			3472	3472	free OH
2D	745	3241	1214	199	ν_1 [N_2O in $(N_2O{\bullet}H_2O)^+$]
			1292	16	ν_1 (solvent N_2O)
			1484	66	H_2O bending
			2066	455	ν_3 [N_2O in $(N_2O{\bullet}H_2O)^+$]
			2245	372	ν_3 (solvent N_2O)
			2986	1739	H-bonded OH
			3470	371	free OH

[a] The correction with the zero point vibrational energy is performed to obtain these values.
[b] A scaling factor of 0.9464 is employed for the calculated frequencies.

Table 3. Relative energies, binding energies, vibrational frequencies, IR intensities, and assignment for optimized isomers of $[(N_2O)_3H_2O]^+$.

isomer	Relative Energy[a] (cm^{-1})	Binding Energy[a] (cm^{-1})	Frequency[b] (cm^{-1})	IR intensity (km/mol)	Assignment
3A	(0)	2725[c]	1156	125	ν_1 [N_2O in $(N_2O•H_2O)^+$]
			1219	253	ν_1 (solvent N_2O)
			1221	135	
			1479	54	H_2O bending
			2139	117	ν_3 [N_2O in $(N_2O•H_2O)^+$]
			2245	561	ν_3 (solvent N_2O)
			2249	342	
			3057	2320	H-bonded OH
			3124	1943	
3B	71	2654[c]	1157	125	ν_1 [N_2O in $(N_2O•H_2O)^+$]
			1219	194	ν_1 (solvent N_2O)
			1323	25	
			1482	52	H_2O bending
			2142	128	ν_3 [N_2O in $(N_2O•H_2O)^+$]
			2247	517	ν_3 (solvent N_2O)
			2264	740	
			3033	2388	H-bonded OH
			3110	1996	
3C	162	2645[d]	1157	124	ν_1 [N_2O in $(N_2O•H_2O)^+$]
			1323	33	ν_1 (solvent N_2O)
			1323	17	
			1485	50	H_2O bending
			2144	138	ν_3 [N_2O in $(N_2O•H_2O)^+$]
			2260	1082	ν_3 (solvent N_2O)
			2266	527	
			3026	2437	H-bonded OH
			3089	2074	
3D	738	2732[e]	1217	242	ν_1 [N_2O in $(N_2O•H_2O)^+$]
			1220	155	ν_1 (solvent N_2O)
			1292	15	
			1477	47	H_2O bending
			2091	575	ν_3 [N_2O in $(N_2O•H_2O)^+$]
			2245	532	ν_3 (solvent N_2O)
			2249	339	
			3048	2280	H-bonded OH
			3117	1870	

[a] The correction with the zero point vibrational energy is performed to obtain these values.
[b] A scaling factor of 0.9464 is employed for the calculated frequencies.
[c] The fragment species are isomer 2A and N_2O.

[d]The fragment species are isomer 2C and N_2O.
[e]The fragment species are isomer 2D and N_2O.

Table 4. Binding energy, vibrational frequencies, IR intensities, and assignment for an optimized isomer of $[(N_2O)_4H_2O]^+$.

Isomer	Binding Energy[a] (cm^{-1})	Frequency[b] (cm^{-1})	IR intensity (km/mol)	
4A	1775[c]	1160	94	ν_1 [N_2O in $(N_2O•H_2O)^+$]
		1222	218	ν_1 (solvent N_2O)
		1224	267	
		1238	125	
		1489	77	H_2O bending
		2133	140	ν_3 [N_2O in $(N_2O•H_2O)^+$]
		2215	203	ν_3 (solvent N_2O)
		2244	521	
		2247	628	
		3135	5276	H-bonded OH
		3230	1701	

[a] The correction with the zero point vibrational energy is performed to obtain these values.
[b] A scaling factor of 0.9464 is employed for the calculated frequencies.
[c] The fragment species are isomer 3A and N_2O.

FIGURE CAPTIONS

Figure 1. The IRPD spectra of $[(N_2O)_nH_2O]^+$ ions with n = 2–7 in the 1100–3800 cm^{-1} region.

Figure 2. Expanded views of the IRPD spectra for $[(N_2O)_nH_2O]^+$ (n = 2–7) in the (a) 1100–1400 and (b) 2000–2300 cm^{-1} regions.

Figure 3. (a, b) The optimized structures of the $(N_2O \cdot H_2O)^+$ ion calculated at the B3LYP/6-311++G(d,p) level of theory. Numbers in the figure are the distance of the intermolecular bond drawn with dashed lines in Å unit. Numbers in parentheses represent the charge distribution on the constituent molecules. ΔE stands for the total energy (cm^{-1}) relative to that of the most stable isomer (1A). The total energy is corrected by the zero-point vibrational energy. (c) A representative of the bonding MOs of 1A formed between the N_2O and H_2O components.

Figure 4. (a) The IRPD spectrum of the $[(N_2O)_2H_2O]^+$ ion. (b–e) The structures and the IR spectra of stable isomers (2A–2D) for the $[(N_2O)_2H_2O]^+$ ion Numbers in parentheses show the charge distribution on the constituent molecules. The solid and dotted curves are the IR spectra reproduced by using Lorentzian components with a full width at half maximum (fwhm) of 20 cm^{-1}.

Figure 5. (a) The IRPD spectrum of the $[(N_2O)_3H_2O]^+$ ion. (b–e) The structures and the IR spectra of stable isomers (3A–3D) for the $[(N_2O)_3H_2O]^+$ ion. Numbers in parentheses show the charge distribution on the constituent molecules. The

solid and dotted curves are the IR spectra reproduced by using Lorentzian components with a fwhm of 20 cm^{-1}.

Figure 6. (a) The IRPD spectrum of the $[(N_2O)_4H_2O]^+$ ion. (b) The structure and the IR spectrum of a stable isomer (4A), which as a component similar to isomer 3A. Numbers in parentheses show the charge distribution on the constituent molecules. The solid and dotted curves are the IR spectra reproduced by using Lorentzian components with a fwhm of 20 cm^{-1}.

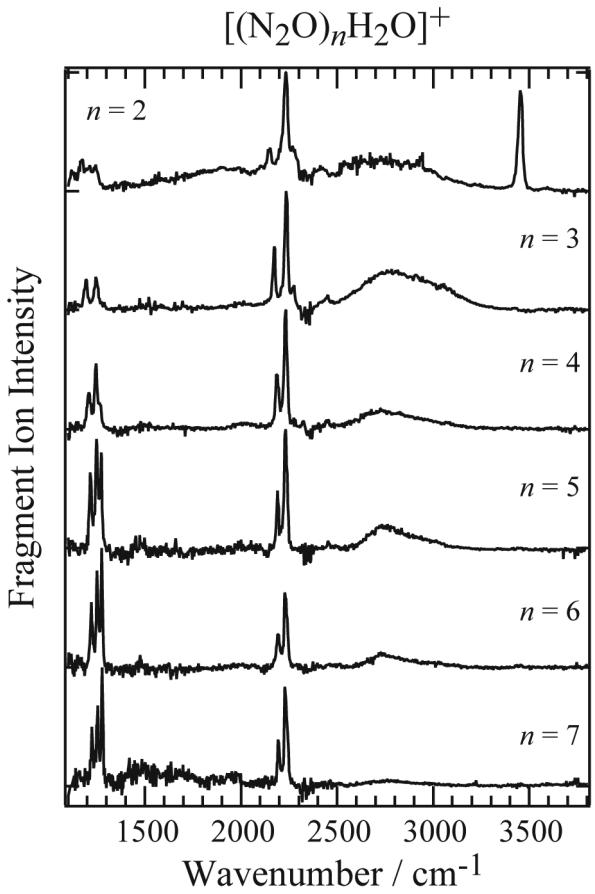

Figure 1. Matsushima et al.

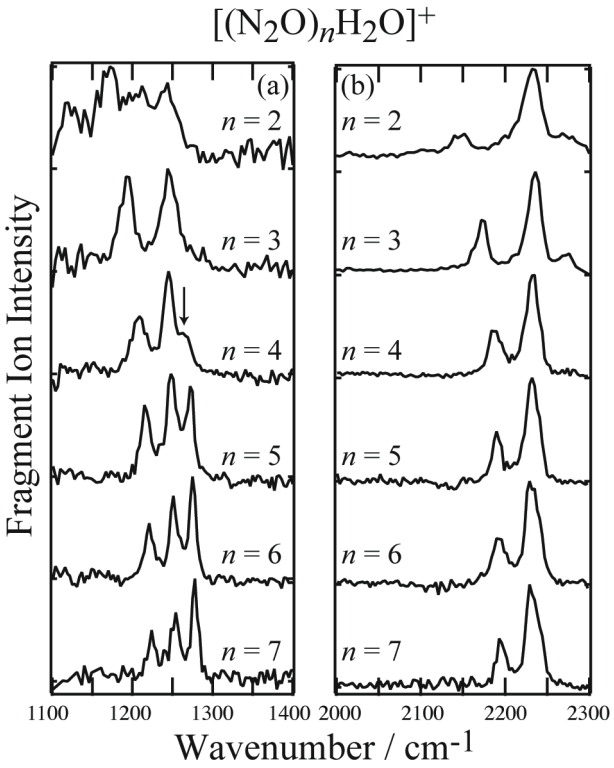

Figure 2. Matsushima et al.

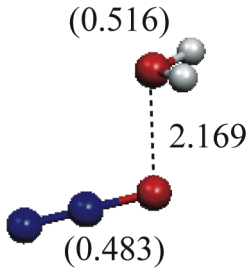

(a) 1A (ΔE = 0 cm^{-1})

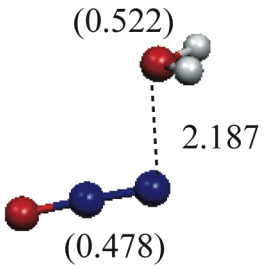

(b) 1B (ΔE = 760 cm^{-1})

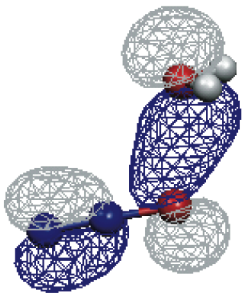

(c) 1A

Figure 3. Matsushima et al.

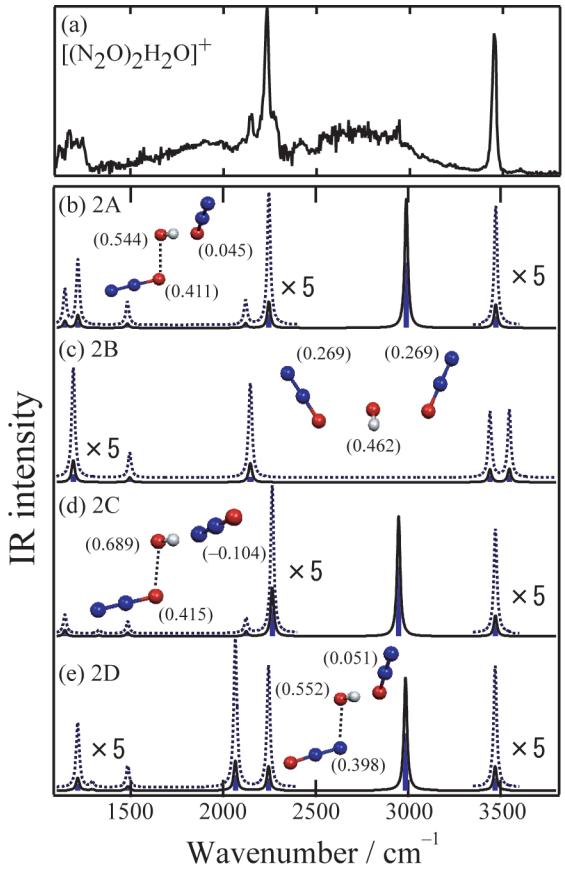

Figure 4. Matsushima et al.

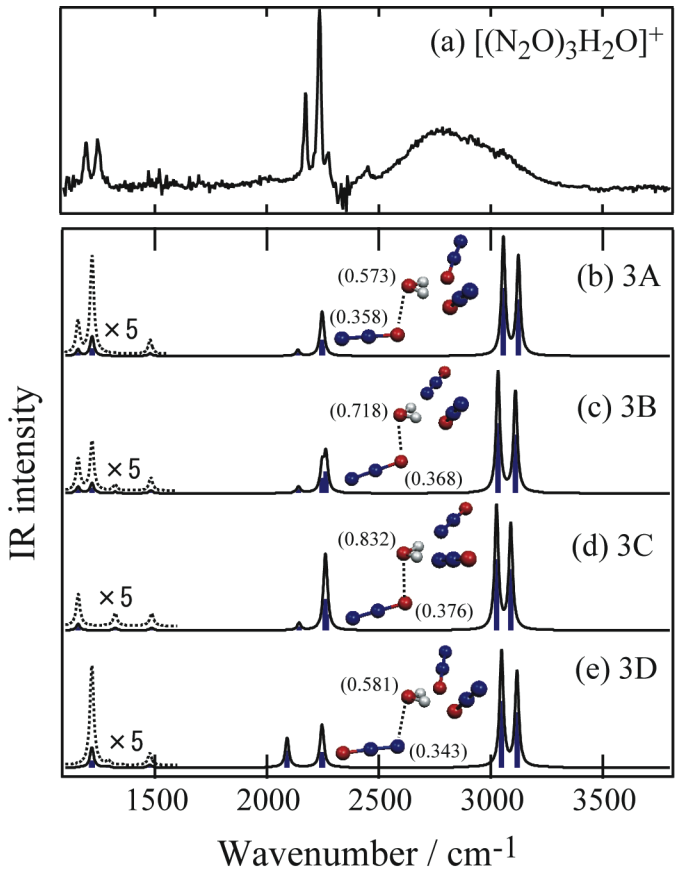

Figure 5. Matsushima et al.

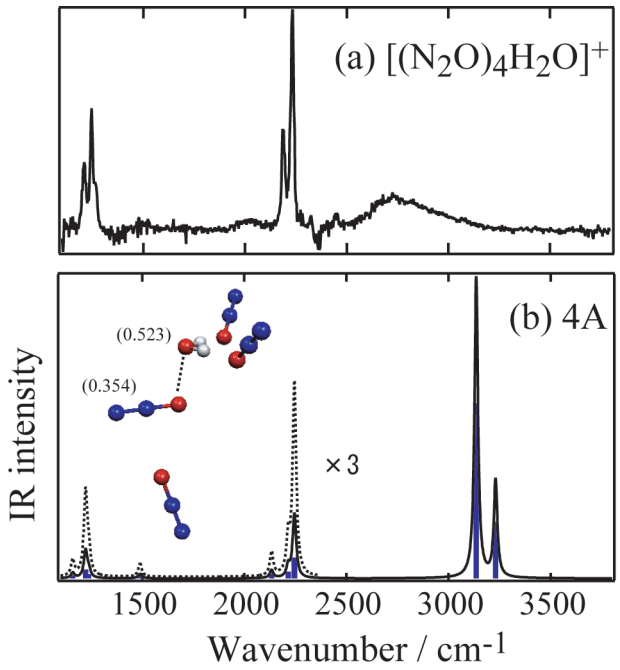

Figure 6. Matsushima et al.